IOP Publishing Journal of Physics A: Mathematical and Theoretical
J. Phys. A: Math. Theor. **54** (2021) 445701 (15pp) https://doi.org/10.1088/1751-8121/ac284f

Solitary waves with intensity-dependent dispersion: variational characterization

D E Pelinovsky[1,2,*], R M Ross[3] and P G Kevrekidis[3]

[1] Department of Mathematics and Statistics, McMaster University, Hamilton, Ontario, L8S 4K1, Canada
[2] Department of Applied Mathematics, Nizhny Novgorod State Technical University, Nizhny Novgorod, 603950, Russia
[3] Department of Mathematics and Statistics, University of Massachusetts, Amherst, MA 01003-4515, United States of America

E-mail: dmpeli@math.mcmaster.ca

Received 14 June 2021, revised 12 September 2021
Accepted for publication 20 September 2021
Published 7 October 2021

Abstract

A continuous family of singular solitary waves exists in a prototypical system with intensity-dependent dispersion. The family has a cusped soliton as the limiting lowest energy state and is formed by the solitary waves with bell-shaped heads of different lengths. We show that this family can be obtained variationally by minimization of mass at fixed energy and fixed length of the bell-shaped head. We develop a weak formulation for the singular solitary waves and prove that they are stable under perturbations which do not change the length of the bell-shaped head. Numerical simulations confirm the stability of the singular solitary waves.

Keywords: solitary waves, nonlinear Schrodinger equation, intensity-dependent dispersion, variational characterization, Lyapunov stability

(Some figures may appear in colour only in the online journal)

1. Introduction

Dispersive nonlinear systems typically feature the interplay of dispersion and nonlinearity that is prototypically represented through the well-known model of the nonlinear Schrödinger (NLS) equation [1, 2]. This interplay is responsible for the formation of smooth solitary waves in a wide class of dispersive nonlinear systems. Nevertheless, some physical systems feature intensity-dependent dispersion (IDD); relevant examples include the femtosecond pulse propagation in quantum well waveguides [3], the electromagnetically induced transparency in coherently prepared multistate atoms [4], and fiber-optics communication systems [5]. Such

*Author to whom any correspondence should be addressed.

features have been discussed in the context of both photonic and phononic (acoustic) crystals [6] and have even been argued to arise at the quantum-mechanical level (between Fock states) in the work of [7].

Our focus here is in addressing the NLS model with the prototypical IDD introduced in the context of nonlinear optics in [5]:

$$\mathrm{i}\psi_t + (1 - |\psi|^2)\psi_{xx} = 0, \tag{1}$$

where $\psi = \psi(x, t)$ is the complex wave function. The dispersion coefficient in the prototypical IDD model (1) is linearly proportional to the intensity $I := |\psi|^2$ and changes sign at the normalized unit intensity.

It was shown in [5] that the NLS equation (1) admits formally two conserved quantities:

$$Q(\psi) = -\int_{\mathbb{R}} \log\,|1 - |\psi|^2|\,\mathrm{d}x, \qquad E(\psi) = \int_{\mathbb{R}} |\psi_x|^2\,\mathrm{d}x. \tag{2}$$

The two conserved quantities have the meaning of the mass and energy of the optical system. The conserved quantities (2) are defined in the subspace of H^1 functions given by

$$X = \left\{ u \in H^1(\mathbb{R}) : \quad \left| \int_{\mathbb{R}} \log\,|1 - |\psi|^2|\,\mathrm{d}x \right| < \infty \right\}, \tag{3}$$

which is the energy space of the NLS equation (1).

Existence and stability of solitary waves in dispersive nonlinear models are subjects that attract much attention due to their importance in understanding the global nonlinear dynamics of such models. For instance, soliton and multi-soliton solutions were investigated in the NLS equation under Wick-type stochastic effects [8]. Higher-order (e.g., with the fourth order dispersion) variants of the NLS model were examined as regards their breather solutions and their applications in birefringent fibers [9]. Analytical solutions for the modified NLS equation were derived and studied in the context of quantum waves on lattices [10].

Solitary waves of the NLS equation (1) were first considered in [5] where existence of a single bell-shaped soliton was shown by qualitative approximations. In our previous work [11], we showed that this bell-shaped soliton is a member of a continuous family of singular solitary waves which are different from each other as concerns the length of the bell-shaped heads. The limiting solution of this family is the cusped soliton with zero length of the bell-shaped head.

Solitary waves of the NLS equation (1) are the standing wave solutions of the form $\psi(x, t) = \mathrm{e}^{\mathrm{i}\omega t} u(x)$ with real ω and $u(x)$ (without loss of generality) satisfying formally the nonlinear differential equation

$$\omega u = (1 - u^2)u''(x) \tag{4}$$

subject to the decay to zero at infinity. Since the classical solutions to the differential equation (4) are singular at the points of x where $u(x) = \pm 1$, solitary waves have to be defined in a weak formulation. One definition of weak solutions was used in [11] (see definition 1 below); however, this definition was not useful for the proof of orbital stability of the solitary waves in the NLS equation (1).

In the present work, we revisit this problem and propose a weak formulation which enables us to establish a notion of Lyapunov stability of the singular solitary waves in the NLS equation (1). The theoretical results are corroborated with the direct numerical simulations of the NLS equation (1). The methods and results obtained in this work are similar to the recent studies of compactons in the degenerate NLS equation [12] and in the sublinear KdV equation [13].

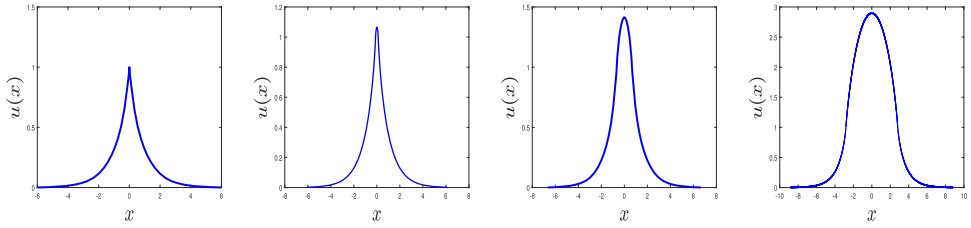

Figure 1. The spatial profiles of four single-humped solitary wave solutions of the second-order equation (4) for $\omega = 1$. From left to right: $C = -\infty$ (cusped soliton), $C = -1$, $C = 0$, and $C = 1$.

Our presentation is structured as follows. In section 2, we present the mathematical background, basic definitions of the problem, and state the main theorems. In section 3, we prove the main results, while in section 4, we illustrate them with numerical simulations. Finally, in section 5, we briefly summarize our findings.

2. Mathematical setup and main results

We start with the definition of weak solutions of the differential equation (4) which was introduced in [11].

Definition 1. We say that $u \in H^1(\mathbb{R})$ is a weak solution of the differential equation (4) if it satisfies the following equation

$$\omega\langle u, \varphi\rangle + \langle (1-u^2)u', \varphi'\rangle - 2\langle u(u')^2, \varphi\rangle = 0, \quad \text{for every } \varphi \in H^1(\mathbb{R}), \tag{5}$$

where $\langle \cdot, \cdot \rangle$ is the standard inner product in $L^2(\mathbb{R})$.

The weak solutions are obtained as parts of the smooth orbits of the second-order differential equation (4). The smooth orbits satisfy the first-order invariant in the form

$$\frac{1}{2}\left(\frac{\mathrm{d}u}{\mathrm{d}x}\right)^2 + \frac{\omega}{2}\log|1-u^2| = C, \tag{6}$$

where the value of C is constant along every smooth orbit. It was proven in [11] that a continuous family of weak solutions exists for each $\omega > 0$. The family describes positive and single-humped solitary waves shown on figure 1. The phase portrait computed from the energy levels C is shown on figure 2. None of the solitary wave solutions on figure 1 exist in the exact analytic form. Their construction is achieved by using the smooth orbits on the phase plane shown on figure 2 and glued together.

The exponentially decaying tails of the solitary waves correspond to the level $C = 0$, whereas the head of the bell-shaped solitary waves corresponds to an arbitrarily fixed value of C. The limiting cusped soliton satisfying $0 < u(x) \leqslant 1$ represents the lowest energy state in the family and corresponds formally to the limit $C \to -\infty$. The bell-shaped solitary wave for different values of $C \in \mathbb{R}$ has the head located in the interval $[-\ell_C, \ell_C]$, where $1 < u(x) \leqslant \sqrt{1+\mathrm{e}^{2C}}$ for $x \in (-\ell_C, \ell_C)$. The tails and the head of the bell-shaped solitary waves are connected at the points $x = \pm\ell_C$, where $u(\pm\ell_C) = 1$ and $u'(\pm\ell_C)$ diverge.

With the precise analysis of the asymptotic behavior of the solutions near the singularities (similar to [14]), we have proven in [11] that the solutions satisfy the weak formulation in

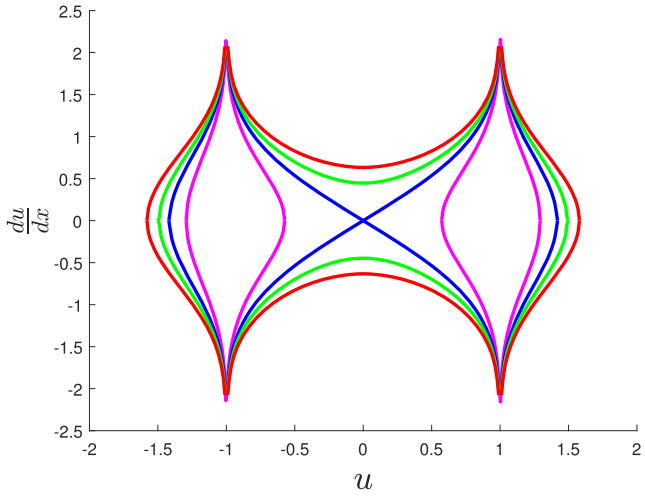

Figure 2. The phase portrait computed from the level curves (6).

definition 1 and belong to the energy space X. The following theorem gives the summary of results obtained in [11] under the normalization $\omega = 1$.

Theorem 1. *Fix $\omega = 1$. There exists a continuous family of weak, positive, and single-humped solutions of definition 1 parametrized by $C \in \mathbb{R}$ such that*

$$u_C(x) = \begin{cases} u_{\text{head},C}(x), & x \in [-\ell_C, \ell_C], \\ u_{\text{cusp}}(|x| - \ell_C), & |x| > \ell_C, \end{cases} \tag{7}$$

where ℓ_C is uniquely defined by

$$\ell_C := \int_1^{\sqrt{1+\mathrm{e}^{2C}}} \frac{\mathrm{d}u}{\sqrt{2C - \log(u^2-1)}}, \tag{8}$$

$u_{\text{head},C}(x)$ for $x \in [-\ell_C, \ell_C]$ is defined implicitly by

$$\ell_C - |x| = \int_1^u \frac{\mathrm{d}\xi}{\sqrt{2C - \log(\xi^2-1)}}, \quad u \in (1, \sqrt{1+\mathrm{e}^{2C}}], \tag{9}$$

and $u_{\text{cusp}}(x)$ for $x \in \mathbb{R}$ is defined implicitly by

$$|x| = \int_u^1 \frac{\mathrm{d}\xi}{\sqrt{-\log(1-\xi^2)}}, \quad u \in (0,1). \tag{10}$$

Moreover, $u_C \in X \subset H^1(\mathbb{R})$ with the following singular behavior as $|x| \to \ell_C$:

$$u_C(x) = 1 + (\ell_C - |x|)\sqrt{|\log|\ell_C - |x|||}\left[1 + \mathcal{O}\left(\frac{\log|\log|\ell_C - |x|||}{|\log|\ell_C - |x|||}\right)\right], \tag{11}$$

where $\mathcal{O}(v)$ denotes a C^1 function of v at either side of $v = 0$.

The purpose of this work is to develop the variational characterization of the solitary wave solutions of theorem 1 in order to prove their Lyapunov stability with respect to small perturbations. In order to place the solutions in the variational context and to deal with the singularity of the solitary wave solutions, we have to use a new definition of weak solutions.

Definition 2. Fix $L > 0$ and define

$$X_L := \{u \in X : \quad u(x) > 1, \quad x \in (-L, L) \quad \text{and} \quad u(x) \leqslant 1, \quad |x| \geqslant L\}. \tag{12}$$

Pick $u_L \in X_L$ satisfying

$$\lim_{|x| \mapsto L} \frac{u_L(x) - 1}{(L - |x|)\sqrt{|\log|L - |x||}} = 1.$$

We say that $u \in X_L \subset H^1(\mathbb{R})$ is a weak solution of the differential equation (4) if it satisfies the following equation

$$\langle u', \varphi' \rangle + \omega \langle (1 - u^2)^{-1} u, \varphi \rangle = 0, \quad \text{for every } \varphi \in H^1_L, \tag{13}$$

where $H^1_L := \left\{\varphi \in H^1(\mathbb{R}) : (1 - u_L^2)^{-1}\varphi \in L^2(\mathbb{R}) \cap L^\infty(\mathbb{R})\right\}$.

The standard way to characterize smooth solitary waves in the NLS equation is to look for minimizers of energy $E(u)$ at fixed mass $Q(u)$ [15]. However, lemmas 1–3 (proven by using methods developed in [16, 17]) show that the mappings $C \mapsto \ell_C$ and $C \mapsto E(u_C)$ are monotone whereas the mapping $C \mapsto Q(u_C)$ is non-monotone. As a result, *we develop a novel variational characterization of the singular solitary waves by looking at minimizers of mass $Q(u)$ at fixed energy $E(u)$*.

The stationary equation (4) is the Euler–Lagrange equation for the action functional

$$\Lambda_\omega(u) = Q(u) + \omega^{-1} E(u), \tag{14}$$

where $Q(u)$ and $E(u)$ are the conserved mass and energy of the NLS equation (1) given by (2). Expanding of $\Lambda_\omega(u)$ at $u \in X_L$ with the test function $\varphi \in H^1_L$ yields

$$\begin{aligned}\Lambda_\omega(u + \varphi) - \Lambda_\omega(u) = 2\langle (1 - u^2)^{-1} u, \varphi \rangle + 2\omega^{-1} \langle u', \varphi' \rangle \\ + \mathcal{O}(\|\varphi'\|_{L^2}^2 + \|(1 - u^2)^{-1}\varphi\|_{L^2 \cap L^\infty}^2).\end{aligned} \tag{15}$$

The first variation of Λ_ω vanishes if $u \in X_L$ is the weak solution of definition 2, hence the corresponding weak solution is a critical point of $\Lambda_\omega(u)$ in X_L. In order to characterize this critical point, we consider the constrained minimization problem

$$\mathcal{Q}_{\mu,L} := \inf_{u \in X_L} \{Q(u) : E(u) = \mu\}. \tag{16}$$

If u is the minimizer of the constrained problem (16), then the Lyapunov stability theory implies that it is orbitally stable in the time evolution of the NLS equation (1).

In the context of the variational problem (16), the parameter $\omega > 0$ serves as the Lagrange multiplier and the parameter $L > 0$ defines the support of the head of the solitary wave as in definition 2. The solitary wave is weakly singular at $x = \pm L$.

The following theorem formulates the main result of the paper. The proof of this theorem relies on the monotonicity of the mappings $C \mapsto \ell_C$ and $C \mapsto E(u_C)$ (lemmas 1 and 2), an

elementary scaling argument (lemma 4), and convexity of the second variation of the action functional $\Lambda_\omega(u)$ (lemma 5).

Theorem 2. *For every $\mu > 0$ and $L > 0$, there exists a ground state, that is, the minimizer of the constrained variational problem (16) in X_L. The minimizer coincides with a rescaled version of u_C in theorem 1 for some $C = C_{\mu,L}$.*

Remark 1. The result of theorem 2 implies the Lyapunov stability of the solitary wave solutions of theorem 1 under perturbations which do not change the length of the bell-shaped head. Stability of the solitary waves is confirmed in the numerical simulations of the time-dependent NLS equation (1) reported in section 4.

Remark 2. The cusped soliton $u_{\rm cusp}$ can be included in the statement of theorem 2 in the formal limit $L \to 0$ and $C_{\mu,L} \to -\infty$. It is also a minimizer of mass at fixed E in the class of functions

$$X_0 := \{u \in X : u(0) = 1 \quad \text{and} \quad u(x) < 1, \quad x \neq 0\}. \tag{17}$$

This implies Lyapunov stability of the cusped soliton under perturbations in X_0.

3. Proof of theorem 2

The following three lemmas address monotonicity of the mappings $C \mapsto \ell_C$, $C \mapsto E(u_C)$, and $C \mapsto Q(u_C)$. The proofs are based on the following standard property from vector calculus. If $W(u,v)$ is a C^1 function in an open region of $\mathbb{R}^2$, then the differential of W is defined by

$$\mathrm{d}W(u,v) = \frac{\partial W}{\partial u}\,\mathrm{d}u + \frac{\partial W}{\partial v}\,\mathrm{d}v$$

and the line integral of $\mathrm{d}W(u,v)$ along any C^1 contour γ connecting two points (u_0,v_0) and (u_1,v_1) does not depend on γ and is evaluated as

$$\int_\gamma \mathrm{d}W(u,v) = W(u_1,v_1) - W(u_0,v_0).$$

A similar study of the monotonicity of the period function in the context of differential equations on quantum graphs was recently developed in [16, 17].

Lemma 1. *Fix $\omega = 1$ and consider the solitary wave solutions of theorem 1 parametrized by $C \in \mathbb{R}$. The mapping $C \mapsto \ell_C$ is C^1 and monotonically increasing such that $\ell_C \to 0$ as $C \to -\infty$ and $\ell_C \to \infty$ as $C \to +\infty$.*

Proof. In order to show that the mapping $C \mapsto \ell_C$ is C^1 and to compute $\frac{\mathrm{d}\ell_C}{\mathrm{d}C}$, we regularize the integral formula (8) by using the first-order invariant (6) with $\omega = 1$:

$$\begin{aligned} C\ell_C &= \int_1^{\sqrt{1+\mathrm{e}^{2C}}} \frac{C\,\mathrm{d}u}{\sqrt{2C - \log(u^2-1)}} \\ &= \frac{1}{2}\int_1^{\sqrt{1+\mathrm{e}^{2C}}} \left[\sqrt{2C - \log(u^2-1)} + \frac{\log(u^2-1)}{\sqrt{2C - \log(u^2-1)}}\right] \mathrm{d}u. \end{aligned}$$

Denote $A(u) := \log(u^2 - 1)$ and write $v^2 + A(u) = 2C$ for the integral curve at the constant level C. Since $A'(u) \neq 0$ for $u > 1$, we have

$$\begin{aligned} \mathrm{d}\left[\frac{A(u)v}{A'(u)}\right] &= \left(1 - \frac{A(u)A''(u)}{[A'(u)]^2}\right) v\,\mathrm{d}u + \frac{A(u)}{A'(u)}\,\mathrm{d}v \\ &= \left(1 - \frac{A(u)A''(u)}{[A'(u)]^2}\right) v\,\mathrm{d}u - \frac{A(u)}{2v}\,\mathrm{d}u. \end{aligned}$$

Therefore, the expression for $C\ell_C$ can be written in the non-singular form

$$\begin{aligned} 2C\ell_C &= \int_1^{\sqrt{1+\mathrm{e}^{2C}}} \left[3 - \frac{2A(u)A''(u)}{[A'(u)]^2}\right] v\,\mathrm{d}u \\ &= \int_1^{\sqrt{1+\mathrm{e}^{2C}}} \left[3 + \frac{1+u^2}{u^2}\,\log(u^2-1)\right] v\,\mathrm{d}u, \end{aligned}$$

where we have used that $v = 0$ at $u = \sqrt{1 + \mathrm{e}^{2C}}$ and $\lim\limits_{u\to 1}(u^2 - 1)|\log(u^2 - 1)|^{3/2} = 0$. Since the right-hand side is a C^1 function of C, it follows that the mapping $C \mapsto \ell_C$ is C^1 so that differentiation in C yields

$$2C\frac{\mathrm{d}\ell_C}{\mathrm{d}C} = \int_1^{\sqrt{1+\mathrm{e}^{2C}}} \left[1 + \frac{1+u^2}{u^2}\,\log(u^2-1)\right] \frac{\mathrm{d}u}{v},$$

where we have used that $1 = v\frac{\partial v}{\partial C}$ at fixed u. Let us now integrate by parts with the use of

$$\begin{aligned} \frac{\mathrm{d}}{\mathrm{d}u}\left[\frac{u^2-1}{u}\sqrt{2C - \log(u^2-1)}\right] &= -\frac{1}{\sqrt{2C - \log(u^2-1)}} \\ &\quad + \frac{1+u^2}{u^2}\sqrt{2C - \log(u^2-1)}. \end{aligned}$$

Substituting it to the formula for $2C\frac{\mathrm{d}\ell_C}{\mathrm{d}C}$ and canceling $2C$ on both sides of equation yields the final expression

$$\frac{\mathrm{d}\ell_C}{\mathrm{d}C} = \int_1^{\sqrt{1+\mathrm{e}^{2C}}} \frac{(1+u^2)\mathrm{d}u}{u^2\sqrt{2C - \log(u^2-1)}}, \tag{18}$$

which shows that $\frac{\mathrm{d}\ell_C}{\mathrm{d}C} > 0$. The limit $\ell_C \to 0$ as $C \to -\infty$ follows from the fact that both the integrand and the length of integration in (8) converge to zero as $C \to -\infty$. On the other hand, the length of integration in (8) diverges as e^C whereas the integrand converges to zero as $C^{-1/2}$ if $C \to \infty$, so that $\ell_C \to \infty$ as $C \to \infty$. □

Lemma 2. *In the setting of lemma 1, the mapping $C \mapsto E(u_C)$ is C^1 and monotonically increasing such that $E(u_C) \to E(u_{\text{cusp}})$ as $C \to -\infty$ and $E(u_C) \to \infty$ as $C \to +\infty$.*

Proof. It follows from (7) that

$$E(u_C) = E(u_{\text{cusp}}) + 2\int_1^{\sqrt{1+\mathrm{e}^{2C}}} \sqrt{2C - \log(u^2-1)}\mathrm{d}u, \tag{19}$$

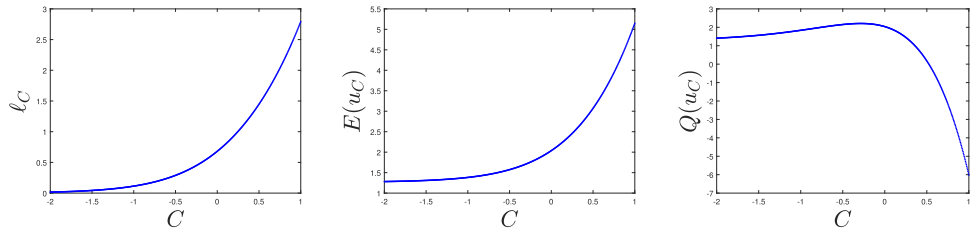

Figure 3. Dependencies of ℓ_C (left), $E(u_C)$ (middle), and $Q(u_C)$ (right) versus C.

where the right-hand side is C^1 in C. Differentiating of (19) in C yields

$$\frac{\mathrm{d}E(u_C)}{\mathrm{d}C} = 2\int_1^{\sqrt{1+\mathrm{e}^{2C}}} \frac{\mathrm{d}u}{\sqrt{2C - \log(u^2-1)}} = 2\ell_C, \tag{20}$$

which shows that $\frac{\mathrm{d}E(u_C)}{\mathrm{d}C} > 0$. The length of integration in the second integral in (19) for $E(u_C)$ converges to 0 as e^{2C} as $C \to -\infty$ whereas the integrand grows like $|C|^{1/2}$ as $C \to -\infty$. Hence the second integral in (19) converges to 0 and $E(u_C) \to E(u_{\text{cusp}})$ as $C \to -\infty$. On the other hand, both the length of integration and the integrand in (19) grow as $C \to +\infty$ so that $E(u_C) \to \infty$ as $C \to \infty$. □

Lemma 3. *In the setting of lemma 1, the mapping $C \mapsto Q(u_C)$ is C^1 and there exist $C_1 \leqslant C_2 < 0$ such that*

$$\frac{\mathrm{d}}{\mathrm{d}C}Q(u_C) > 0, \quad C \in (-\infty, C_1) \quad \text{and} \quad \frac{\mathrm{d}}{\mathrm{d}C}Q(u_C) < 0, \quad C \in (C_2, \infty). \tag{21}$$

Proof. It follows from (7) that

$$Q(u_C) = Q(u_{\text{cusp}}) - 2\int_1^{\sqrt{1+\mathrm{e}^{2C}}} \frac{\log(u^2-1)}{\sqrt{2C - \log(u^2-1)}}\,\mathrm{d}u, \tag{22}$$

By using (6), this expression can be rewritten as

$$Q(u_C) = Q(u_{\text{cusp}}) - 4C\ell_C + E(u_C) - E(u_{\text{cusp}}), \tag{23}$$

where the right-hand side is C^1 in C due to lemmas 1 and 2. Differentiating of (23) in C and using (20) yield

$$\frac{\mathrm{d}Q(u_C)}{\mathrm{d}C} = -2\ell_C - 4C\frac{\mathrm{d}\ell_C}{\mathrm{d}C}. \tag{24}$$

It follows from positivity of (18) that $\frac{\mathrm{d}Q(u_C)}{\mathrm{d}C} < 0$ for $C \geqslant 0$. On the other hand, it follows from (22) that $Q(u_C) > Q(u_{\text{cusp}})$ for sufficiently large negative C. Hence, there exist $C_1 \leqslant C_2 < 0$ such that the signs in (21) hold. □

Remark 3. Figure 3 shows all three mappings as functions of C. It suggests that the mapping $C \mapsto Q(u_C)$ has exactly one critical point, that is, $C_1 = C_2$ in the statement of lemma 3. We were not able to prove this property from the analysis of (24).

The following lemma uses the scaling transformation to obtain a critical point of the constrained variational problem (16).

Lemma 4. *For every $\mu > 0$ and $L > 0$, there exists a unique value of $C = C_{\mu,L}$ such that a critical point of the constrained variational problem* (16) *is defined by the solution u_C of theorem* 1.

Proof. Let u_C be the solitary wave solution of the normalized equation

$$u = (1 - u^2)\, u''(x). \tag{25}$$

The scaled function $u_\omega(x) = u_C(\sqrt{\omega}x)$ is a solution of the second-order equation (4) for $\omega > 0$ and is the critical point of the action functional $\Lambda_\omega(u)$ given by (14) in X_L. Using the scaling transformation in the conserved mass and energy in (2) gives

$$Q(u_\omega) = \frac{1}{\sqrt{\omega}} Q(u_C), \quad E(u_\omega) = \sqrt{\omega} E(u_C).$$

The singularities of u_ω are located at

$$L = \frac{1}{\sqrt{\omega}} \ell_C.$$

The Lagrange multiplier ω is selected from the condition $\mu = E(u_\omega) = \sqrt{\omega} E(u_C)$. Computing the Jacobian of the transformation $(\omega, C) \mapsto (\mu, L)$ by

$$\begin{vmatrix} \frac{\partial \mu}{\partial \omega} & \frac{\partial \mu}{\partial C} \\ \frac{\partial L}{\partial \omega} & \frac{\partial L}{\partial C} \end{vmatrix} = \frac{1}{2\omega} \left[E(u_C) \frac{\mathrm{d}\ell_C}{\mathrm{d}C} + \ell_C \frac{\mathrm{d}E(u_C)}{\mathrm{d}C} \right], \tag{26}$$

it follows by lemmas 1 and 2 that the Jacobian is positive for every $C \in \mathbb{R}$. Hence the mapping $(\omega, C) \mapsto (\mu, L)$ is invertible and there exists a unique $C = C_{\mu,L}$ for every $\mu > 0$ and $L > 0$. □

Remark 4. If $L = 0$, then $\ell_C = 0$ in the formal limit $C \to -\infty$. This yields the cusped soliton u_{cusp} with $\sqrt{\omega} = \frac{\mu}{E(u_{\text{cusp}})}$ for every $\mu > 0$. Hence the limiting value $L = 0$ can be included in the statement of lemma 4 with $\lim_{L \to 0} C_{\mu,L} = -\infty$ for fixed $\mu > 0$.

Remark 5. If $\mu = 0$, then $E(u_\omega) = 0$ with the only solution $u_\omega(x)$ being a constant. If the constant is nonzero, then $u_\omega \notin H^1(\mathbb{R})$. If the constant is zero, then L is not defined. In either case, the limiting value $\mu = 0$ cannot be included in the statement of lemma 4.

Remark 6. The inverse transformation of the mapping $(\omega, C) \mapsto (\mu, L)$ in the proof of lemma 4 can be made explicit. Since $\sqrt{\omega} = \frac{\ell_C}{L}$ and $\mu = \sqrt{\omega} E(u_C)$, C is uniquely found from the equation $\ell_C E(u_C) = L\mu$. Hence, $C_{\mu,L} \equiv C_{\mu L}$ depends on one parameter μL. This dependence is shown in figure 4.

The following lemma states that the critical point of lemma 4 is in fact a strict local minimizer of the constrained variational problem (16).

Lemma 5. *Fix $\omega = 1$ and $C \in \mathbb{R}$. The solution u_C of theorem* 1 *is a strict local minimizer of the action functional $\Lambda_{\omega=1}(u)$ in $X_{L=\ell_C}$.*

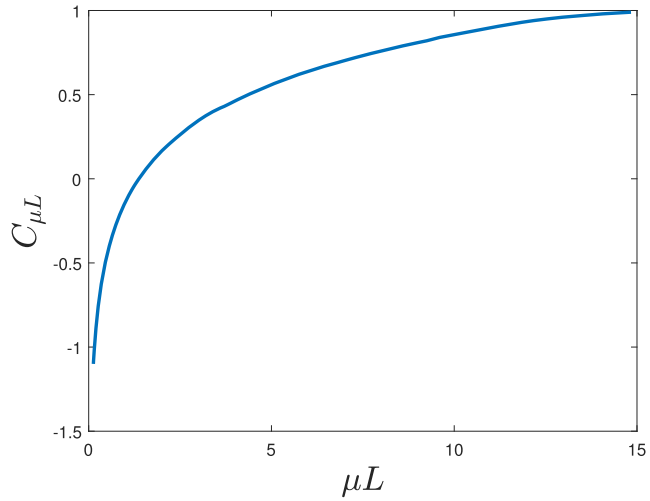

Figure 4. Dependence of $C_{\mu L}$ from lemma 4 on the parameter μL.

Proof. Let $u_C \in X_{\ell_C} \subset H^1(\mathbb{R})$ be a solitary wave solution of the normalized equation (25). Let $v + \mathrm{i}w$ with real $v, w \in H^1_{\ell_C} \subset H^1(\mathbb{R})$ be a perturbation to u_C. Since u_C satisfies (11) in theorem 1, we have $(1-u_C^2)^{-1}v, (1-u_C^2)^{-1}w \in L^\infty(\mathbb{R})$ and $u_C(\pm\ell_C) = 1$ so that $v(\pm\ell_C) = w(\pm\ell_C) = 0$.

Expanding $\Lambda_{\omega=1}(u_C + v + \mathrm{i}w)$ in powers of (v, w) and integrating by parts for $\int_{\mathbb{R}} u_C'(x)v'(x)\mathrm{d}x$ with $v(\pm\ell_C) = 0$ and $(1-u_C^2)^{-1}v \in L^\infty(\mathbb{R})$ yields a vanishing linear term in (v, w) because u_C is the critical point of the action functional $\Lambda_{\omega=1}(u)$, see expansion (15). Continuing the expansion to the quadratic and higher orders in (v, w) yields the following expansion

$$\Lambda_{\omega=1}(u_C + v + \mathrm{i}w) = \Lambda_{\omega=1}(u_C) + Q_+(v) + Q_-(w) + R(v, w), \tag{27}$$

where Q_+ and Q_- are the quadratic forms given by

$$Q_+(v) = \int_{\mathbb{R}} \left[(v_x)^2 + \frac{(1+u_C^2)v^2}{(1-u_C^2)^2} \right] \mathrm{d}x$$

and

$$Q_-(w) = \int_{\mathbb{R}} \left[(w_x)^2 + \frac{w^2}{1-u_C^2} \right] \mathrm{d}x,$$

whereas $R(v, w)$ is the remainder term given by

$$R(v, w) = -\int_{\mathbb{R}} \left[\log\left(1 - \frac{2u_C v + v^2 + w^2}{1-u_C^2}\right) + \frac{2u_C v}{1-u_C^2} + \frac{(1+u_C^2)v^2}{(1-u_C^2)^2} + \frac{w^2}{1-u_C^2} \right] \mathrm{d}x.$$

The quadratic forms $Q_\pm$ and the remainder term $R(v, w)$ are bounded since $v, w \in H^1(\mathbb{R})$ and $(1-u_C^2)^{-1}v, (1-u_C^2)^{-1}w \in L^2(\mathbb{R}) \cap L^\infty(\mathbb{R})$ are small for the perturbation terms v, w. In particular, it follows from Taylor's expansion of the logarithmic function that there exists a positive constant C such that

$$|R(v,w)| \leqslant C\|(1-u_C^2)^{-1}v\|_{L^2\cap L^\infty}^3 + C\|(1-u_C^2)^{-1}w\|_{L^2\cap L^\infty}^3,$$

so that the remainder term is cubic with respect to the small perturbation terms $v, w \in H^1_{\ell_C}$.

We claim that there exist $C_\pm > 0$ such that

$$Q_\pm(v) \geqslant C_\pm \|v\|_{H^1}^2, \quad v \in H^1_{\ell_C} \subset H^1(\mathbb{R}), \tag{28}$$

hence the quadratic forms are strictly positive and u_C is a strict local minimizer of the action functional $\Lambda_{\omega=1}(u)$ in $X_{L=\ell_C}$ by the second derivative test.

It remains to prove the bounds (28). Since $v(\pm\ell_C) = w(\pm\ell_C) = 0$, the domain $\mathbb{R}$ is partitioned to $(-\infty,-\ell_C)\cup(-\ell_C,\ell_C)\cup(\ell_C,\infty)$ and each quadratic form is considered separately in each interval subject to the Dirichlet boundary condition at $x = \pm\ell_C$.

Since $0 < u_C(x) \leqslant \sqrt{1+\mathrm{e}^{2C}}$, we have

$$\frac{1+u_C^2}{(1-u_C^2)^2} \geqslant \min(1, \mathrm{e}^{-4C}),$$

hence the bound (28) holds for Q_+ with $C_+ := \min(1,\mathrm{e}^{-4C})$.

Since $(1-u_C^2)^{-1}$ is sign-indefinite, special treatment is needed for Q_-. On each interval of the partition $\mathbb{R} = (-\infty,-\ell_C)\cup(-\ell_C,\ell_C)\cup(\ell_C,\infty)$, the quadratic form Q_- can be expressed in terms of the differential operator L_- given by

$$L_- = -\partial_x^2 + \frac{1}{1-u_C^2}. \tag{29}$$

The spectral problem for L_- is set on $(-\infty,-\ell_C)$, $(-\ell_C,\ell_C)$, and (ℓ_C,∞) subject to the Dirichlet conditions at $x = \pm\ell_C$. This defines the spectrum of L_- in $L^2((-\infty,-\ell_C)\cup(-\ell_C,\ell_C)\cup(\ell_C,\infty))$ with the domain $H_0^2(-\infty,-\ell_C)\cap H_0^2(-\ell_C,\ell_C)\cap H_0^2(\ell_C,\infty)$, where the subscript in H_0^2 indicates the Dirichlet conditions at the corresponding points.

On the other hand, L_- can also be considered in $L^2(\mathbb{R})$ with a suitably defined domain in $L^2(\mathbb{R})$. Since $u_C(x)\to 0$ as $|x|\to\infty$ exponentially fast, Weyl's theorem implies that the essential spectrum of L_- in $L^2(\mathbb{R})$ is located on $[1,\infty)$. Since $L_-u_C = 0$ with $u_C \in H^1(\mathbb{R})$ and $u_C(x) > 0$ for every $x\in\mathbb{R}$, Sturm's theorem implies that the discrete spectrum of L_- in $L^2(\mathbb{R})$ is located in $[0,1)$ and 0 is a simple eigenvalue of L_- in $L^2(\mathbb{R})$.

When L_- is restricted on $L^2((-\infty,-\ell_C)\cup(-\ell_C,\ell_C)\cup(\ell_C,\infty))$ subject to the Dirichlet conditions at $x=\pm\ell_C$, the smallest eigenvalue of L_- is no longer zero because $u_C(\pm\ell_C) = 1 \neq 0$. By Rayleigh–Ritz theorem, the smallest eigenvalue of L_- in $L^2((-\infty,-\ell_C)\cup(-\ell_C,\ell_C)\cup(\ell_C,\infty))$ is strictly positive, and it yields $C_- > 0$ in the bound (28) for Q_-. □

Remark 7. For the cusped soliton with $\ell_C = 0$ as $C\to-\infty$, the bounds (28) hold with $C_\pm = 1$ since $0 < u(x) \leqslant 1$ for all $x\in\mathbb{R}$. Hence it is not necessary to partition $\mathbb{R}$ into $(-\infty,0)\cup(0,\infty)$ for the proof of these bounds for the cusped soliton.

We are now ready to prove theorem 2.

By lemma 4, for every $\mu > 0$ and $L > 0$, the critical point of the constrained variational problem (16) is given by $u_\omega(x) = u_C(\sqrt{\omega}x)$ with uniquely defined $C = C_{\mu L}$ and $\omega = \left[\frac{\ell_{C_{\mu L}}}{L}\right]^2$. By lemma 5, this critical point is a local minimizer of the action functional $\Lambda_\omega(u)$. From theorem 1, no other critical points satisfying the Euler–Lagrange equation (13) exist in X_L. Therefore, the critical point is the global minimizer of mass $Q(u)$ for fixed energy $E(u) = \mu$. The proof extends to $\mu > 0$ and $L = 0$ with u_{cusp} replacing u_C by remarks 4 and 7.

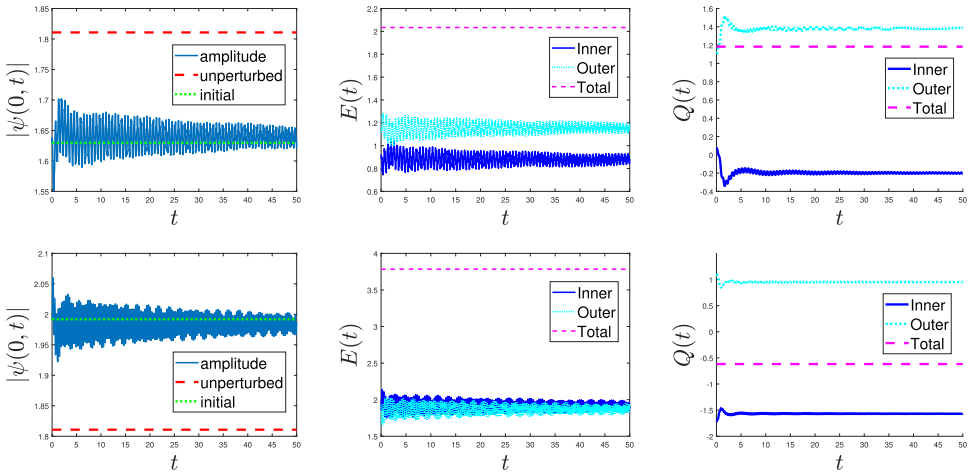

Figure 5. Amplitude (left), energies (middle) and masses (right) for the time evolution of the initial condition (30) with $C = 0$ (the bell-shaped soliton), where $P = 0.9$ (top) and $P = 1.1$ (bottom). In the amplitude figures, the green dotted line represents the amplitude of the initial condition, while the red dashed one represents the amplitude of the unperturbed soliton.

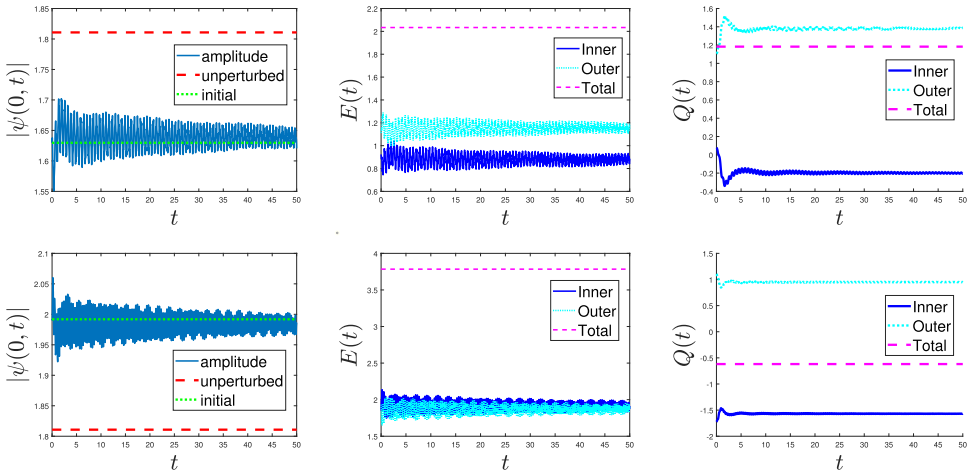

Figure 6. The same as figure 5 but for $C = 0.5$.

4. Time evolution of perturbations

In order to corroborate the results regarding the existence and stability of the minimizer of the constrained variational problem (16), we investigate the time evolution of perturbations of the solitary wave with the profile u_C for some uniquely selected $C = C_{\mu L}$. We consider perturbations of the singular solitary waves which do not alter the singularity location at $\pm L$ with $L = \ell_C$, in line with our theoretical analysis, but change the energy level $E(u_C) = \mu$. We do this by perturbing only the head portion of the solitary wave on $(-\ell_C, \ell_C)$, while leaving the

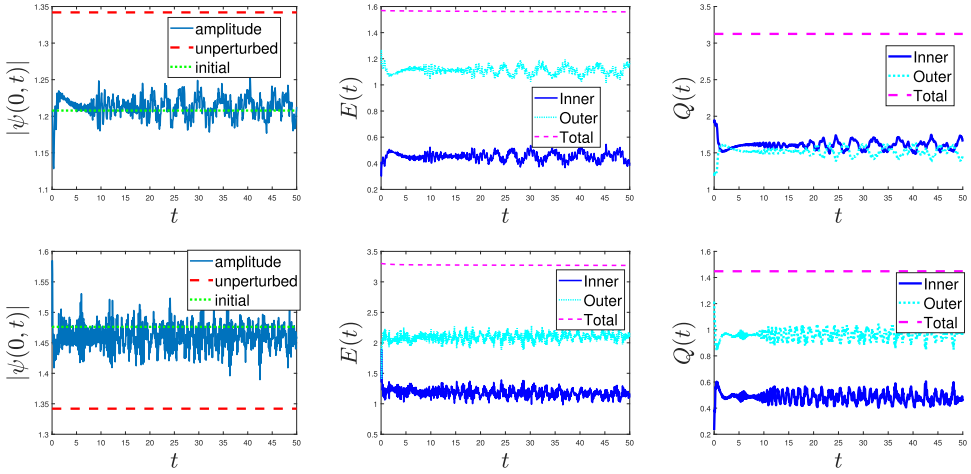

Figure 7. The same as in figure 5 but for $C = -0.5$.

solution in the outer regions unchanged. The initial condition is given by

$$u_P(x) = \begin{cases} Pu_{C,\text{head}}(x), & |x| < \ell_C \\ u_{\text{cusp}}(|x| - \ell_C), & |x| \geqslant \ell_C \end{cases}, \tag{30}$$

where the perturbation factor P is close to 1, both for $P > 1$, e.g., $P = 1.1$, and for $P < 1$, e.g., $P = 0.9$.

To perform the time evolution of the NLS equation (1), we use a pseudospectral method. First, we discretize the interval $[-500, 500]$ with $N = 2000$ points. Next, spatial derivatives ψ_x and ψ_{xx} on the grid are approximated by vectors $D_1\psi$ and $D_2\psi$ respectively, where D_1 and D_2 are matrix representations of the first and second derivative operators based on the circulant matrices from [18]. Finally, time integration is performed using the fourth-order Runge–Kutta method, with time step $\Delta t = 0.001$.

At each time t in the evolution, we compute the energy contained in the inner and outer portions, given by

$$E_{\text{inner}}(t) = \int_{-L}^{L} |\psi_x(x,t)|^2 \, \mathrm{d}x, \tag{31}$$

$$E_{\text{outer}}(t) = \int_{|x|>L} |\psi_x(x,t)|^2 \, \mathrm{d}x, \tag{32}$$

as well as the mass

$$Q_{\text{inner}}(t) = -\int_{-L}^{L} \log|\,1 - |\psi(x,t)|^2| \, \mathrm{d}x, \tag{33}$$

$$Q_{\text{outer}}(t) = -\int_{|x|>L} \log|\,1 - |\psi(x,t)|^2| \, \mathrm{d}x. \tag{34}$$

These give insight into how energy and mass may be exchanged between the inner and outer regions. We also plot the value at the peak $|\psi(0,t)|$. Figures 5–7 show these diagnostics for three members of the solitary wave family (i.e. $C = 0$, $C = 0.5$ and $C = -0.5$) with two

perturbation factors at $P = 0.9$ and $P = 1.1$ (top and bottom panels in each figure, respectively). In all the simulations, we observe slowly decaying oscillations around a different solitary wave near the initial perturbation, suggesting that the singular solitary waves are stable in the time evolution of the NLS equation (1). This agrees with the Lyapunov stability of the solitary wave solutions which follow from the result of theorem 2.

A closer inspection of the amplitude of the wave points to a very slow (presumably power law) decay toward a new solitary wave equilibrium. Additionally, in our (total) energy and mass conserving simulations, we observe a very weak exchange of energy and mass between the inner (head) and the outer regions of the solitary wave. The latter may be affected by the approximate nature of the numerical computations, e.g., by the numerical approximation of the unit modulus at $x = \pm\ell_C$.

We remark that, due to numerical limitations, we are not able to investigate perturbations which change the singularity locations at $\pm L$ while keeping the same energy level μ. In theory, the location of the singularity for these perturbations may change in time, because ψ_{xx} is infinite when $|\psi| = 1$, and the term $(1 - |\psi|^2)\psi_{xx}$ in the NLS equation (1) is indeterminate. In numerical simulations, however, the derivative ψ_{xx} is replaced by a finite approximation, which results in the term $(1 - |\psi|^2)\psi_{xx}$ being computed as 0 when $|\psi| = 1$, in which case the NLS equation (1) implies that the singularity locations at $\pm L$ are preserved in the time evolution.

5. Conclusions

In the present work, we have provided a variational characterization of solitary waves in a prototypical NLS model with IDD. We have argued that minimization of mass at fixed energy and fixed length of the bell-shaped head is beneficial from an analytical point of view since it allows us to establish Lyapunov stability of the singular solitary waves. This expected stability of the solitary waves was confirmed by direct dynamical simulations of the NLS model. We have observed in numerical simulations that perturbations of such waveforms lead to a slow relaxation of perturbed solitary waves to a new solitary wave within the family.

Among further open problems, we mention the rigorous analysis of well-posedness of the NLS model in the energy space where the solitary waves exist. It is also interesting to investigate how the singularity locations can change in the time evolution of the solitary waves; our analytical and numerical results rely on the fixed location of the singularities. Finally, it is interesting to study Lyapunov stability of other (sign-changing) solitary waves and periodic solutions discussed both in [5, 11]. It is also worth exploring generalizations of the NLS model in the settings of the discrete (waveguide) systems, as well as in higher-dimensional systems. Such studies are deferred to future publications.

Acknowledgments

D E Pelinovsky acknowledges financial support from the state task program in the sphere of scientific activity of the Ministry of Science and Higher Education of the Russian Federation (Task No. FSWE-2020-0007) and from the grant of the president of the Russian Federation for the leading scientific schools (Grant No. NSH-2485.2020.5). P G Kevrekidis acknowledges financial support by the National Science Foundation under Grant No. PHY-2110030 and under Grant No. DMS-1809074.

Data availability statement

The data generated and/or analysed during the current study are not publicly available for legal/ethical reasons but are available from the corresponding author on reasonable request.

ORCID iDs

D E Pelinovsky https://orcid.org/0000-0001-5812-440X
P G Kevrekidis https://orcid.org/0000-0002-7714-3689

References

[1] Sulem C and Sulem P L 1999 *The Nonlinear Schrödinger Equation* (New York: Springer)
[2] Fibich G 2015 *The Nonlinear Schrödinger Equation: Singular Solutions and Optical Collapse* (New York: Springer)
[3] Koser A A, Sen P K and Sen P 2009 Effect of intensity dependent higher-order dispersion on femtosecond pulse propagation in quantum well waveguides *J. Mod. Opt.* **56** 1812–8
[4] Greentree A D, Richards D, Vaccaro J A, Durant A V, de Echaniz S R, Segal D M and Marangos J P 2003 Intensity-dependent dispersion under conditions of electromagnetically induced transparency in coherently prepared multistate atoms *Phys. Rev.* A **67** 023818
[5] Lin C-Y, Chang J-H, Kurizki G and Lee R-K 2020 Solitons supported by intensity-dependent dispersion *Opt. Lett.* **45** 1471–4
[6] Mankeltow K, Leamy M J and Ruzzene M 2013 Comparison of asymptotic and transfer matrix approaches for evaluating intensity-dependent dispersion in nonlinear photonic and phononic crystals *Wave Motion* **50** 494–508
[7] Kirchmair G *et al* 2013 Observation of quantum state collapse and revival due to the single-photon Kerr effect *Nature* **495** 205–9
[8] Han H-B, Li H-J and Dai C-Q 2021 Wick-type stochastic multi-soliton and soliton molecule solutions in the framework of nonlinear Schrödinger equation *Appl. Math. Lett.* **120** 107302
[9] Du Z, Tian B, Qu Q-X, Chai H-P and Zhao X-H 2020 Vector breathers for the coupled fourth-order nonlinear Schrödinger system in a birefringent optical fiber *Chaos Solitons Fractals* **130** 109403
[10] Luo J 2021 Exact analytical solution of a novel modified nonlinear Schrödinger equation: solitary quantum waves on a lattice *Stud. Appl. Math.* **146** 550–62
[11] Ross R M, Kevrekidis P G and Pelinovsky D E 2021 Localization in optical systems with an intensity-dependent dispersion *Q. Appl. Math.* **79** 641–65
[12] Germain P, Harrop-Griffiths B and Marzuola J L 2020 Compactons and their variational properties for degenerate KdV and NLS in dimension 1 *Q. Appl. Math.* **78** 1–32
[13] Pelinovsky D E, Slunyaev A V, Kokorina A V and Pelinovsky E N 2021 Stability and interaction of compactons in the sublinear KdV equation *Commun. Nonlinear Sci. Numer. Simul.* **101** 105855
[14] Alfimov G L, Korobeinikov A S, Lustri C J and Pelinovsky D E 2019 Standing lattice solitons in the discrete NLS equation with saturation *Nonlinearity* **32** 3445–84
[15] Weinstein M I 1986 Lyapunov stability of ground states of nonlinear dispersive evolution equations *Commun. Pure Appl. Math.* **39** 51–67
[16] Kairzhan A, Marangell R, Pelinovsky D E and Xiao K L 2021 Standing waves on a flower graph *J. Differ. Equ.* **271** 719–63
[17] Noja D and Pelinovsky D E 2020 Standing waves of the quintic NLS equation on the tadpole graph *Calc. Var. Partial Differ. Equ.* **59** 173
[18] Trefethen N 2000 *Spectral Methods in MatLab* (Philadelphia, PA: SIAM)